

An Electron Localization Function (ELF) Study of the 2-Norbornyl Cation[†]

Nick H. Werstiuk,* Heidi M. Muchall, and Stéphane Noury

Department of Chemistry, McMaster University, Hamilton, Ontario L8S 4M1, Canada

Received: May 31, 2000; In Final Form: October 4, 2000

Wave functions obtained at Becke3LYP, Becke3PW91, MP2, and QCISD levels of theory for the 2-norbornyl cation (**1**) are used in a topological analysis of the Becke–Edgecombe electron localization function (ELF) with the Silvi suite of programs. Partitioning of the molecular space of the cation into basins of attractors yields information on the shared valence basin interactions at the C1–C2–C6 face of **1** and other C_s species in which the C1–C6 and C2–C6 distances are increased incrementally to 193.5 pm. At the Becke3LYP/cc-PVTZ//Becke3LYP/cc-PVTZ level, a single trisynaptic basin with a population of 0.83 electrons connects C1 and C2 to C6 in the optimized geometry where the C1/C2–C6 distances are 188.9 pm. When the C1/C2–C6 distances are increased by 4.5 pm to 193.5 pm, the shared trisynaptic basin splits into a monosynaptic basin at C6 with a population of 0.49 electrons and a disynaptic basin between C1 and C2 with a population of 2.75 electrons; and ΔE_T is only 0.12 kcal mol⁻¹. Disynaptic basins with electron populations in the region of 0.5 electrons link C1–C6 and C2–C6 in the equilibrium optimized geometries of **1** obtained at the MP2, Becke3PW91, and QCISD levels (the C1/C2–C6 distances range from 182.5 to 184.6 pm). This is the case even when the large correlation-consistent basis set cc-PVTZ is used to obtain the wave functions. But these shared interactions are lost when the C1/C2–C6 distances are increased in the range of 8 pm. While the nature of the basins at the C1–C2–C6 face depends on the C1/C2–C6 distances and the basis set, on the whole, increases in energy only ranging up to 0.55 kcal mol⁻¹ are found with large basis sets when the distances are increased by 4–8 pm. At the point where the shared valence interactions between C1/C2 and C6 are lost, there is no discontinuity in the calculated total energy. According to our ELF analysis the formation of **1** from the C_s primary “open” cation involves a transfer of electrons from the valence basin of the double bond at C1–C2 to a basin at C6. The stabilization of **1** relative to the open primary cation results from an electrostatic interaction between a carbocation and the electrons of a carbon–carbon double bond.

Introduction

Presently, two topology-based methods are used to study molecular *structure*. In AIM (the quantum theory of atoms in molecules) developed by Richard Bader and co-workers, molecular space is partitioned through an analysis of the gradient vector field of the one-electron density ρ .¹ A bonding interaction between a pair of atoms is indicated by the presence of a (3, -1) critical point (cp) in ρ in the internuclear region. The eigenvector associated with the single positive eigenvalue (curvature) defines a unique pair of trajectories of $\nabla\rho(r)$ which originate at the (3, -1) cp and terminate at the nuclei of the pair of atoms. This pair of trajectories defines an atomic interaction line that corresponds to a bond path in an equilibrium geometry. It is important to understand that “the presence of a bond path provides a universal indicator of bonding between the atoms so connected”.² No bond path, no bonding.

The other method involves a topological analysis of the gradient vector field of the Becke–Edgecombe electron localization function (ELF)³ as implemented by Silvi and co-workers.^{4,5} Within AIM and ELF, basin populations are evaluated by integrating the one-electron density over the volume of the basin Ω_i . In ELF there are basically two types of

basins: core basins are organized around nuclei (with $Z > 2$) providing an inner-atomic-shell-like structure and valence basins occupy the remaining space. Each valence basin is characterized by its synaptic order—the number of cores to which is connected. Thus, valence basins are mono-, di-, and polysynaptic. For example, a C–H bond is characterized by a disynaptic basin which encompasses the proton and which shares a common separatrix (surface) with the carbon core basin. A normal C–C bond is characterized by a disynaptic basin which shares two separatrices with the core basins of the carbon atoms, and lone pairs give rise to monosynaptic basins. In the ELF picture, bonding is defined on the basis of how valence basins interact with core basins. That it is important to carry out ELF studies on so-called “nonclassical” carbocations is obvious.

Our modeling studies on the secondary kinetic deuterium isotope effects⁶ observed for solvolysis of *syn*-7- and *anti*-7-chloro-*exo*-2- and *endo*-2-norbornyl brosylates led us eventually to reevaluate the electronic charge distribution of the 2-norbornyl cation (**1**) and initiate a study of the 1,2,4,7-*anti*-tetramethyl-2-norbornyl cation with AIM.^{7,8} These studies revealed that **1** possesses a T-structure—we view it as a π -complex—at the C1–C2–C6 face, in which a cation interacts with a double bond and carbon atom C6 is tetracoordinate. The 1,2,4,7-*anti*-tetramethyl-2-norbornyl cation is found to be a tertiary cation stabilized by hyperconjugation, not a bridged species. In a following paper, we employed AIM to provide further proof

* To whom correspondence may be addressed. Tel: (905) 525-9140. Fax: (905) 522-2509. E-mail: werstiuk@mcmaster.ca.

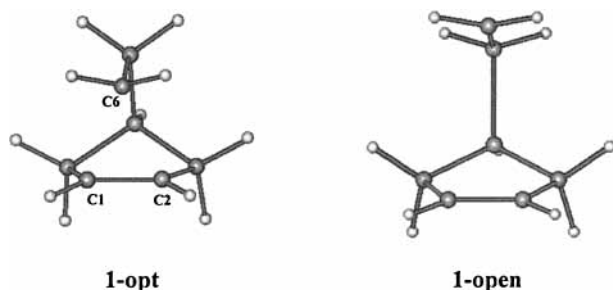
[†] Presented at the 27th Ontario-Quebec Physical Organic Mini-Symposium, Guelph, Ontario, Canada, November 1999.

that the 2-norbornyl cation (**1**) has a T-structure and established what it takes to reach the so-called “nonclassical” bridged structure where bond paths link C1 and C2 to C6.⁹

This paper documents the results of an ELF study on **1** and a number of species in which the C1–C6 and C2–C6 distances are increased incrementally up to 193.5 pm from the equilibrium distance at the Becke3LYP, Becke3PW91, MP2, and QCISD levels of theory.

Computational Details

Becke3LYP, Becke3PW91, MP2, and QCISD calculations were carried out with Gaussian 94¹⁰ on IBM RS/6000 model 39H, SGI R10000 Impact, and SGI Octane and with Gaussian 98¹¹ on Cray T90 computers. Optimizations were carried out within C_s symmetry restrictions and with C1–C6 and C2–C6 distances fixed as indicated in the tables. Because Becke3LYP handles the crucial “classical” 2-norbornyl cation correctly at a reasonably low computational cost⁶ and the inclusion of polarization functions on the hydrogen atoms was essential for the studies performed, we used the 6-311G(d,p) basis set for Becke3LYP and Becke3PW91 calculations. Becke3PW91 calculations were included in this study because we found that this level of theory yielded C1–C6 and C2–C6 internuclear distances for optimized **1** which were comparable to the values obtained at the MP2(full)/6-311G(d,p) level. Thus, near MP2-(full) geometries are obtained at a substantially lower computational cost. To check the influence of higher levels of theory on the wave function, selected geometries were optimized with Dunning’s correlation consistent basis set cc-PVTZ.¹² Similarly, selected geometries were optimized at the MP2(full)/6-311G-(d,p) and QCISD/6-31G(d,p) levels that took the correlation effects of all electrons into account. All single-point calculations were carried out with Gaussian 98 at the cc-PVTZ level with tight convergence criteria. The total energies reported are uncorrected for zero-point vibrational energies. Given the similarity of the geometries in the crucial region of the potential energy surface, we expected that the inclusion of ZPEs would not alter the relative energies significantly. At any rate, whether the corrected or uncorrected energies are used does not impact on the topological analyses. At all the levels of theory used in this study, AIM finds **1-opt** as a T-structure.



ELF calculations were carried out with ELFBIN, VINCI, and FAST_POP (the Silvi suite of programs) which are used to compute the ELF data, carry out the topological analysis, and integrate the basins, respectively.¹³ Calculations on **1-opt** were carried out with the following grids: (a) dimensions of $15 \times 15 \times 15$ au ($7.94 \times 7.94 \times 7.94$ Å, $794 \times 794 \times 794$ pm) and a step size of 0.100 au; (b) dimensions of $8 \times 4 \times 6$ au ($4.23 \times 2.22 \times 3.18$ Å, $423 \times 222 \times 318$ pm) and a step size 0.050 au. A grid of dimension $17 \times 17 \times 17$ au ($9.00 \times 9.00 \times 9.00$ Å, $900 \times 900 \times 900$ pm) and step size 0.133 au were used for

TABLE 1: Total Energies and ELF Basin Populations of Selected Geometries of the 2-Norbornyl Cation at the Becke3LYP/cc-PVTZ// Becke3LYP/cc-PVTZ Level

C1–C6, C2–C6 distance/pm	E_T /hartrees	ΔE_T /kcal mol ⁻¹	basin (population/electrons)
188.9 ^a	-273.156266	0.0	C1–C2–C6(0.83) ^b C1–C2(2.45)
193.0	-273.156143	+0.077	C1–C2–C6(0.50) ^b C1–C2(2.77)
193.5	-273.156070	+0.12	C6(0.49) ^c C1–C2(2.75)

^a The equilibrium optimized geometry. ^b A trisynaptic basin connecting C1–C2–C6. ^c A monosynaptic basin at C6.

1-open. Calculations with the large grids on **1-opt** and **1-open** yielded total populations of 60.00 electrons. The results of the VINCI calculations are visualized with SciAn¹⁴ and saved as .rgb files. XVIEW is used to convert the .rgb files to color gif files which can be incorporated into documents. The displays of the contour and basin plots are derived from the $15 \times 15 \times 15$ au and $8 \times 4 \times 6$ au grid calculations.

Results and Discussion

At the Becke3LYP/cc-PVTZ level, C_s -symmetrical **1-opt** exhibits C1–C6 and C2–C6 distances (Table 1) of 188.9 pm, identical to the value obtained at the lower level of theory (Becke3LYP/6-311G(d,p)) as listed in Table 2, which is included as Supporting Information. Figure 1a displays the irreducible valence basins and core basins of **1-opt** at an ELF contour value of 0.8 viewed perpendicular to the C1–C2–C6 face. The disynaptic C1–C2 basin is colored yellow. Parts b and c of Figure 1 are displays of the 0.60 and 0.50 contours, respectively. In Figure 1c, the red basin visible below C6 is a trisynaptic valence basin with a population of 0.83 electrons that it is stuck on the C1, C2, and C6 core basins. This is seen in Figure 1d that is a display of the ELF basins viewed in a plane that bisects the core basins of C1, C2, and C6. When the C1–C6 and C2–C6 distances are increased by 4.5 pm to 193.5 pm, the interaction with the C1 and C2 core basins is lost as the trisynaptic valence basin splits into a monosynaptic basin with a population of 0.49 electrons at C6 and a disynaptic basin located between C1 and C2 with a population of 2.75 electrons; the increase in the energy that accompanies these disconnections is insignificantly small at 0.12 kcal mol⁻¹. Figure 1e displays the basins of the 193.5 pm species in the C1, C2, and C6 plane; in Figure 1f, a plot of the 0.7 ELF contour overlays the plot of the basins. While the population of the C1–C2 valence basin increases from 2.45 to 2.75 electrons in going from **1-opt** to the 193.5 pm geometry, the sum of the two basins (the trisynaptic and disynaptic basins of **1-opt** and the monosynaptic and disynaptic basins of the 193.5 pm geometry) remains virtually constant at 3.28 and 3.24 electrons, respectively. It appears that the formation of **1-opt** from the C_s primary “open” cation **1-open** involves a transfer of approximately 0.8 electrons from the valence basin of the double bond at C1–C2 to a basin at C6. Seeking support for this we carried out ELF calculations on the 320 pm geometry (**1-open**) that we take as the open primary cation on the basis of our previous AIM study at the Becke3LYP/6-31G(d,p) level. At the Becke3PW91/cc-PVTZ and Becke3LYP/cc-PVTZ levels the open cations are 32.38 and 25.50 kcal mol⁻¹ higher in energy than **1-opt**. That the C1–C2 valence basins of **1-open** at these levels of theory have populations of 3.21 and 3.20 electrons, respectively, provides support for our analysis regarding the transfer of electrons from

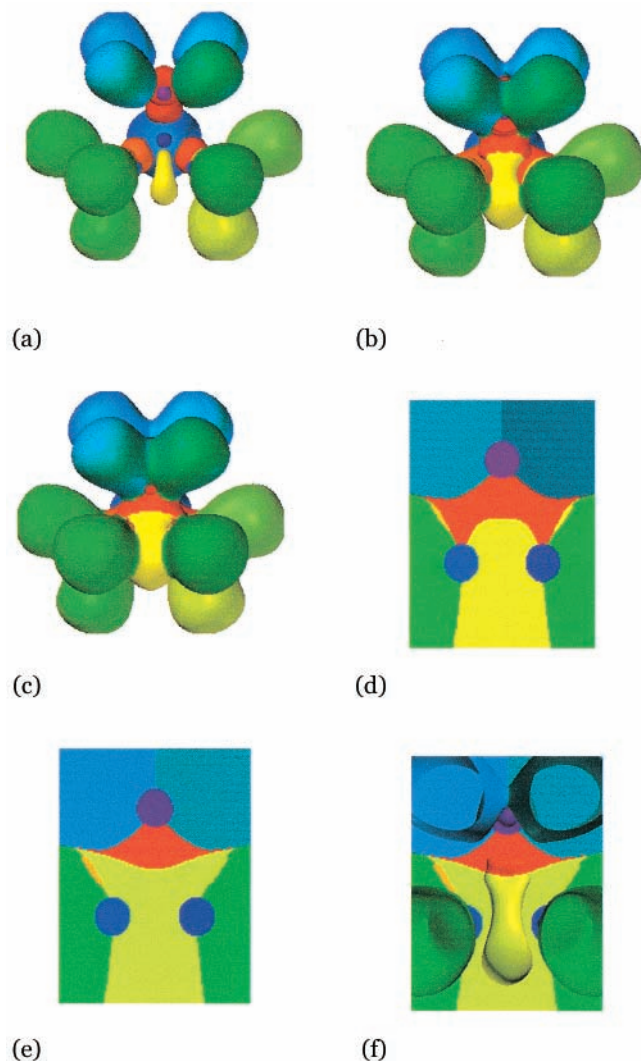


Figure 1. Displays of ELF basins obtained at the Becke3LYP/cc-PVTZ level: (a) the irreducible basins of the Becke3LYP/cc-PVTZ optimized equilibrium geometry **1-opt** at the 0.80 contour viewed perpendicular to the C1–C2–C6 plane; (b) the 0.60 contour of **1-opt**; (c) the 0.50 contour of **1-opt**; (d) in the C1–C2–C6 plane of **1-opt**; (e) in the C1–C2–C6 plane of the 193.5 pm geometry; (f) an overlay plot including the 0.70 ELF contour of the 193.5 pm geometry.

the C1–C2 basin to the basin at C6 of **1-opt**. The results of calculations at the Becke3LYP/6-311G(d,p) level are summarized in Table 2 (included as Supporting Information). With this smaller basis set where electrons are less “delocalized”, the C6–C1–C2 connectivity is not lost until the C1–C6(C2–C6) distance is increased to 193.5 pm (0.5 pm “later” than with the larger basis). Two monosynaptic basins with low electron populations of 0.29 and 0.27 electrons are found connected to C6 (Table 2). We take the fact that there are two monosynaptic basins as an indication that this level of theory is insufficient to describe accurately the valence basins at C6.

At the Becke3PW91/cc-PVTZ level, the C1–C6 and C2–C6 distances (183.6 pm, Table 3) of C_s -symmetrical **1-opt** are midway between the values found at the MP2(full)/6-311G(d,p) (182.6 pm) and QCISD/6-31G(d,p) (184.6 pm) levels but 5.3 pm less than values found with Becke3LYP/cc-PVTZ. Unlike what is found at the Becke3LYP/cc-PVTZ level, separate basins with populations of 0.51 and 0.53 electrons are found in this case. That these basins are stuck on the C1 and C2 core basins is seen in Figure 2a. Figure 2b is a plot of the 0.72 ELF

TABLE 3: Total Energies and ELF Basin Populations of Selected Geometries of the 2-Norbornyl Cation at the Becke3PW91/cc-PVTZ//Becke3PW91/cc-PVTZ Level

C1–C6, C2–C6 distance/pm	E_T / hartrees	ΔE_T / kcal mol ⁻¹	basin (population/ electrons)
183.6 ^a	-273.061134	0.0	C1–C6 (0.51) C2–C6 (0.53) C1–C2(2.32)
190.0	-273.060552	+0.36	C1–C2–C6(0.78) ^b C1–C2(2.49)
191.0	-273.060365	+0.48	C1–C2–C6(0.60) ^c C1–C2(2.66)
191.5	-273.060264	+0.55	C6(0.54) ^d C1–C2(2.74)

^a The equilibrium optimized geometry. ^b A single basin connects C1–C2–C6. ^c A single basin with loss of connectivity of C6 to C1 and C2 essentially complete. ^d A monosynaptic basin at C6.

contour. This result indicates that the nature of basins connecting C6 to C1 and C2 depends on the distances and the level of theory. These connections are lost between 191.0 and 191.5 pm, and a single monosynaptic basin is formed at C6 with a population of 0.54 electrons. Figure 2c displays the basins in the C1, C2, and C6 plane, and Figure 2d is a plot of the 0.7 ELF contour. Here too, the increase in energy relative to **1-opt** is extremely small at approximately 0.50 kcal mol⁻¹, and there is no discontinuity in the total energy when the connections are lost. At the BeckePW91/6-311G(d,p) level, the C6–C1–C2 connectivity is not lost until the C1–C6(C2–C6) distance is increased by 10 pm to 193.5 pm (data are summarized in Table 4 which is included as Supporting Information). While the increase in energy is 0.84 kcal mol⁻¹, no discontinuity is seen in the total energy when the connectivity is lost.

At the MP2(full)/6-311G(d,p) level, C_s -symmetrical **1-opt** exhibits C1–C6 and C2–C6 distances of 182.8 pm, the smallest values observed in the system; the 191.0 pm species is 0.67 kcal mol⁻¹ higher in energy than **1-opt**. Single-point calculations were carried out on 182.8, 190.0, 190.5, and 191.0 pm MP2 geometries with Becke3LYP/cc-PVTZ and Becke3PW91/cc-PVTZ to obtain total energies, relative energies, wave functions, and ELF basin populations for comparisons with the above studies (Table 5). The Becke3PW91/cc-PVTZ//MP2(full)/6-311G(d,p) relative energies mirror the values obtained at the MP2 level because calculations with Becke3PW91 yield a **1-opt** geometry that closely resembles the one obtained with MP2. As seen at the Becke3PW91/cc-PVTZ level, separate valence basins each with populations in the region of 0.53 electrons connect C1 and C2 with C6 of the slightly tighter MP2 **1-opt**. Figure 2, e and f, displays the in-plane basin plots and 0.70 ELF contours, respectively. In the case of the 190.0 and 190.5 pm geometries, a single valence basin connects C1 and C2 to C6 in accord with what was found at the Becke3PW91/cc-PVTZ level. This again shows that distance is the important factor in the formation of a single valence basin versus two. The connectivity is lost with the formation of a monosynaptic basin populated with 0.57 electrons when the C1–C6 and C2–C6 distances are increased to 191.0 pm. Figure 2, g and h, display the in-plane basin plots and 0.70 ELF contours, respectively. At the Becke3LYP/cc-PVTZ//MP2(full)/6-311G(d,p) level, the connectivity between C1/C2 and C6 is lost in the 190.5 pm species and a single monosynaptic basin with a population of 0.59 electrons not connected to C1 and C2 evolves at C6. As seen in the other cases, the incremental changes in energy are small and no discontinuity is seen in the total energy when the connections to C1 and C2 are lost.

At the QCISD(full)/6-31G(d,p) level, C_s -symmetrical **1-opt**

TABLE 5: Total Energies and ELF Basin Populations of Selected Geometries of the 2-Norbornyl Cation

C1–C6, C2–C6 distance/pm	E_T /hartrees				basin (population/ electrons) ^a
	MP2(full)/ 6-311G(d,p)	Becke3lyp/cc-PVTZ/ /MP2(full)/6-311G(d,p) ^b	Becke3pw91/cc-PVTZ// MP2(full)/6-311G(d,p) ^b	ΔE_T (MP2)/ kcal mol ⁻¹	
182.8	-272.401993	-273.155248(0.00)	-273.060853(0.00)	0.00	C1–C6(0.52, 0.53) C2–C6(0.53, 0.52) C1–C2(2.30, 2.30)
190.0	-272.401162	-273.155855(-0.38)	-273.060272(+0.36)	+0.52	C1(C2)–C6(0.74, 0.78) ^c C1–C2(2.52, 2.48)
190.5	-272.401049	-273.155842(-0.37)	-273.060176(+0.41)	+0.59	C1(C2)–C6(0.59, 0.71) ^c C1–C2(2.67, 2.58)
191.0	-272.400929	273.155105(+0.09)	-273.060082(+0.48)	+0.67	C6(0.55, 0.57) ^d C1–C2(2.70, 2.68)

^a Obtained by analysis of the Becke3LYP/cc-PVTZ and Becke3PW91/cc-PVTZ (in italics) wave functions. The electron populations of the C1–C6, C2–C6, and C1–C2 basins were also obtained by analysis of the MP2(full)/6-311G(d,p) wave functions: 182.8 pm geometry 0.47, 0.47, and 2.37; 191.0 pm geometry 0.25, 0.23, and 2.74. ^b The values in parentheses are the relative energies in kcal mol⁻¹. ^c A trisynaptic basin connects C6 to C1 and C2. ^d A monosynaptic basin at C6.

TABLE 6: Total Energies and ELF Basin Populations of Selected Geometries of the 2-Norbornyl Cation at QCISD/6-31G(d,p)//QCISD/6-31G(d,p)Becke3LYP/cc-PVTZ//QCISD/6-31G(d,p), and Becke3PW91/cc-PVTZ//QCISD/6-31G(d,p) Levels

C1–C6, C2–C6 distance/pm	level of theory	ΔE_T (QCISD) kcal mol ⁻¹	basin (population/ electrons)
184.6	QCISD/6-31G(d,p)//QCISD/6-31G(d,p) ^a	0.00 ^a	C1–C6 (0.47), C2–C6 (0.48), ^d C1–C2 (2.37)
184.6	Becke3lyp/cc-PVTZ//QCISD/6-31G(d,p) ^b		C1–C6 (0.51), C2–C6 (0.49), ^e C1–C2 (2.33)
184.6	Becke3pw91/cc-PVTZ//QCISD/6-31G(d,p) ^c		C1–C6 (0.51), C2–C6 (0.50), ^e C1–C2 (2.33)
191.0	QCISD/6-31G(d,p)//QCISD/6-31G(d,p) ^a	+0.41 ^a	C1–C6 (0.36), C2–C6 (0.38), ^e C1–C2 (2.51)
191.0	Becke3lyp/cc-PVTZ//QCISD/6-31G(d,p) ^b		C6 (0.56), ^{e,f} C1–C2 (2.70)
191.0	Becke3pw91/cc-PVTZ//QCISD/6-31G(d,p) ^c		C6 (0.62), ^{e,g} C1–C2 (2.64)
192.0	QCISD/6-31G(d,p)//QCISD/6-31G(d,p) ^a	+0.53	C6 (0.66), ^g C1–C2 (2.60)
192.0	Becke3lyp/cc-PVTZ//QCISD/6-31G(d,p) ^b		C6 (0.52), ^f C1–C2 (2.73)
192.0	Becke3pw91/cc-PVTZ//QCISD/6-31G(d,p) ^c		C6 (0.52), ^f C1–C2 (2.73)

^a The total energies of the optimized equilibrium, 191.0 pm, 192.0 pm geometries are -272.283 337, -272.282 689, and -272.282 486 hartrees, respectively. ^b The total energies of the optimized equilibrium, 191.0, and 192.0 pm geometries are -273.155 923, -273.156 144, and -273.156 093 hartrees, respectively. ^c The total energies of the optimized equilibrium, 191.0, and 192.0 pm geometries are -273.060 905, -273.060 134, and -273.059 927 hartrees, respectively. ^d Based on analysis of the basins in a 15 × 15 × 15 au grid. ^e Based on analysis of the basins in a 8 × 4 × 6 au grid incorporating C1, C2, and C6. ^f A monosynaptic basin at C6. ^g A trisynaptic basin with marginal contact at C1 and C2.

exhibits C1–C6 and C2–C6 distances (Table 6) of 184.6 pm; the 191.0 and 192.0 pm species are 0.41 and 0.54 kcal mol⁻¹ higher in energy than **1-opt**. Single-point calculations were also carried out on these geometries at the Becke3LYP/cc-PVTZ and Becke3PW91/cc-PVTZ levels to obtain wave functions. The total energies and ELF basin populations are listed in Table 6. Separate basins connecting C1 and C2 with C6 were found at the three levels of theory for **1-opt**. The basins very closely resemble those seen in Figure 2e,f. At the QCISD(full)/6-31G(d,p)//QCISD(full)/6-31G(d,p), two basins with the disconnection between C1 and C6 and C2 and C6 being virtually complete are seen in the 192.0 pm species and ΔE_T is 0.53 kcal mol⁻¹. At the Becke3LYP/cc-PVTZ//QCISD(full)/6-31G(d,p) level these connections are lost in the 191.0 pm geometry with the formation of a single monosynaptic basin populated with 0.56 electrons. At the Becke3PW91/cc-PVTZ//QCISD(full)/6-31G(d,p) level, a single basin (0.62 electrons) with marginal connections to C1 and C2 is found for the 191.0 pm geometry; at this level the connections to C1 and C2 are lost in the 192.0

pm geometry. The basins at the C1–C2–C6 face very closely resemble those seen in Figure 2g,h, and ΔE_T between the 191.0 and 192.0 pm species is 0.13 kcal mol⁻¹.

Conclusions

We have determined the total energies and analyzed the ELF function of the C_s -symmetrical 2-norbornyl cation as a function C1/C2–C6 distance at high levels of theory. Shared covalent interactions between C1, C2, and C6 seen in the ELF analysis do not contribute to the stabilization of the C_s -symmetrical 2-norbornyl cation that is 24–32 kcal mol⁻¹ lower in energy relative to the C_s -symmetrical open primary cation depending on the level of theory. This inconsequential local concentration of pair density is also seen in the plots of the Laplacian of **1-opt** at several levels of theory where $\nabla^2\rho$ is close to zero. Thus, our findings in this case are exactly in accord with the results of our earlier AIM study: the 2-norbornyl cation has a T-structure with no bond paths connecting C1 and C2 to C6.⁹

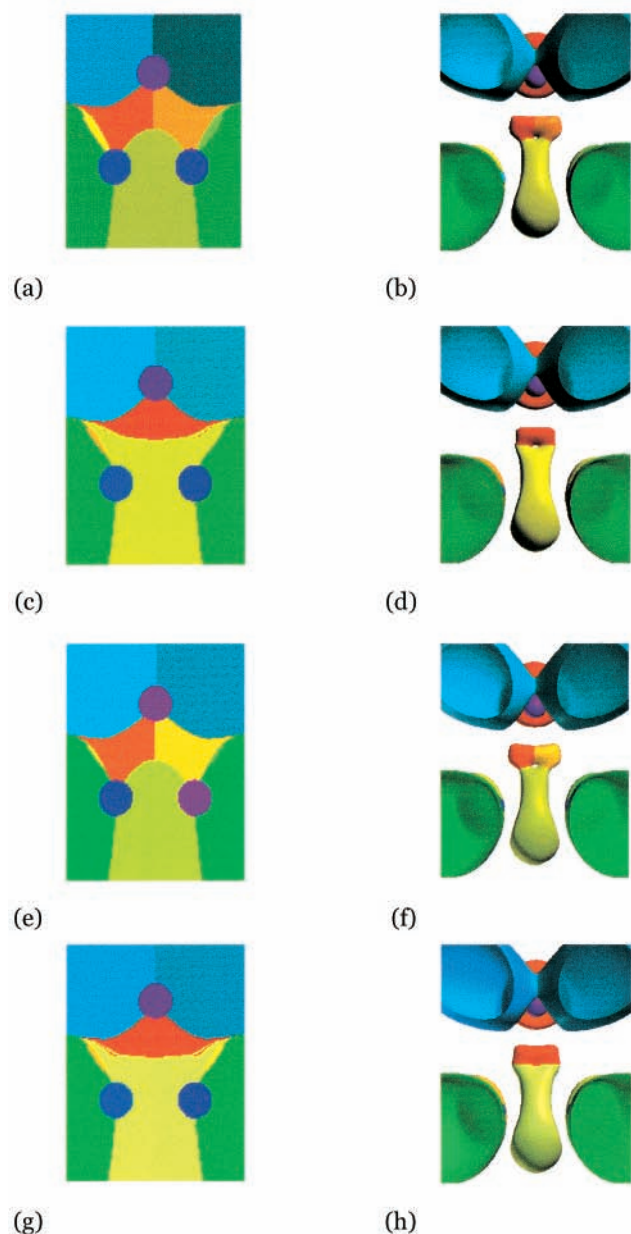


Figure 2. Displays of ELF basins: (a) in the C1–C2–C6 plane of **1-opt** obtained at the BeckePW91/cc-PVTZ level//BeckePW91/cc-PVTZ level; (b) the 0.72 contour of **1-opt** obtained at the BeckePW91/cc-PVTZ level//BeckePW91/cc-PVTZ level; (c) in the C1–C2–C6 plane of 191.5 pm geometry obtained at the BeckePW91/cc-PVTZ level//BeckePW91/cc-PVTZ level; (d) the 0.70 ELF contour of the 191.5 pm geometry obtained at the BeckePW91/cc-PVTZ level//BeckePW91/cc-PVTZ level; (e) in the C1–C2–C6 plane of **1-opt** obtained at the BeckePW91/cc-PVTZ//MP2(full)/6–311(d,p) level; (f) the 0.70 contour of **1-opt** obtained at the BeckePW91/cc-PVTZ//MP2(full)/6–311(d,p) level; (g) in the C1–C2–C6 plane of 191.0 pm geometry obtained at the BeckePW91/cc-PVTZ//MP2(full)/6–311(d,p) level; (h) the 0.70 contour of the 191.0 pm geometry obtained at the BeckePW91/cc-PVTZ//MP2(full)/6–311(d,p) level.

The stabilizing interaction derives from an electrostatic interaction of a carbocation with the electrons of the carbon–carbon

double bond. Thus, the bond path which connects C6 to the (3,–1) C1–C2 bond critical point in the T-structure defines the path of maximum negative potential energy for this interaction. Our work on **1** suggests that ELF studies should be carried out on other so-called “nonclassical” carbocations.

Acknowledgment. We gratefully acknowledge the grant of CPU time on a CRAY T90 vector computer at the NIC at the Research Center Jülich and the usage of the SGI computing installation in the Geochemistry Labs at McMaster funded by the Natural Sciences and Engineering Research Council of Canada (NSERC). We thank NSERC for financial support.

Supporting Information Available: Tables of total energies and basin populations of selected geometries of the 2-norbornyl cation. This material is available free of charge via the Internet at <http://pubs.acs.org>.

References and Notes

- (1) Bader, R. F. W. *Atoms in Molecules. A Quantum Theory*; Clarendon Press: Oxford, UK, 1990.
- (2) Bader, R. F. W. *J. Phys. Chem. A* **1998**, *102*, 7314.
- (3) Becke, A. D.; Edgecombe, K. E. *J. Chem. Phys.* **1990**, *92* 5397.
- (4) Silvi, B.; Savin, A. *Nature* **1994**, *371*, 683.
- (5) Noury, S.; Colonna, F.; Silvi, B. Savin, A. *J. Mol. Struct.* **1998**, *450*, 59.
- (6) Muchall, H. M.; Werstiuk, N. H. *Can. J. Chem.* **1998**, *76*, 1926.
- (7) Werstiuk, N. H.; Muchall, H. M. *J. Mol. Struct. (THEOCHEM)*, **1999**, *463*, 225.
- (8) Muchall, H. M.; Werstiuk, N. H. *J. Phys. Chem. A* **1999**, *103*, 6599.
- (9) Werstiuk, N. H.; Muchall, H. M. *J. Phys. Chem. A* **2000**, *104*, 2054.
- (10) Frisch, M. J.; Trucks, G. W.; Schlegel, H. B.; Gill, P. M. W.; Johnson, B. G.; Robb, M. A.; Cheeseman, J. R.; Keith, T.; Petersson, G. A.; Montgomery, J. A.; Raghavachari, K.; Al-Laham, M. A.; Zakrzewski, V. G.; Ortiz, J. V.; Foresman, J. B.; Peng, C. Y.; Ayala, P. Y.; Chen, W.; Wong, M. W.; Andres, J. L.; Replogle, E. S.; Gomperts, R.; Martin, R. L.; Fox, D. J.; Binkley, J. S.; Defrees, D. J.; Baker, J.; Stewart, J. P.; Head-Gordon, M.; Gonzalez, C.; Pople, J. A. *Gaussian 94*, Revision B.3; Gaussian, Inc.: Pittsburgh, PA, 1995.
- (11) Frisch, M. J.; Trucks, G. W.; Schlegel, H. B.; Scuseria, G. E.; Robb, M. A.; Cheeseman, J. R.; Zakrzewski, V. G.; Montgomery, J. A., Jr.; Stratmann, R. E.; Burant, J. C.; Dapprich, S.; Millam, J. M.; Daniels, A. D.; Kudin, K. N.; Strain, M. C.; Farkas, O.; Tomasi, J.; Barone, V.; Cossi, M.; Cammi, R.; Mennucci, B.; Pomelli, C.; Adamo, C.; Clifford, S.; Ochterski, J.; Petersson, G. A.; Ayala, P. Y.; Cui, Q.; Morokuma, K.; Malick, D. K.; Rabuck, A. D.; Raghavachari, K.; Foresman, J. B.; Cioslowski, J.; Ortiz, J. V.; Baboul, A. G.; Stefanov, B. B.; Liu, G.; Liashenko, A.; Piskorz, P.; Komaromi, I.; Gomperts, R.; Martin, R. L.; Fox, D. J.; Keith, T.; Al-Laham, M. A.; Peng, C. Y.; Nanayakkara, A.; Gonzalez, C.; Challacombe, M.; Gill, P. M. W.; Johnson, B.; Chen, W.; Wong, M. W.; Andres, J. L.; Gonzalez, C.; Head-Gordon, M.; Replogle, E. S.; Pople, J. A. *Gaussian 98*, Revision A.7; Gaussian, Inc.: Pittsburgh, PA, 1998.
- (12) Woon, D. E.; Dunning Jr, T. H. *J. Chem. Phys.* **1993**, *98*, 1358.
- (13) Noury, S.; Krokidis, X.; Fuster, F.; Silvi, B. *Comput. Chem.* **1999**, *23* (6), 597.
- (14) Pepke, E.; Murray, J.; Lyons, J.; Hwu, T.-Y. *SciAn*. Version 1.21 Alpha; Supercomputer Computations Research Institute: Florida State University, Tallahassee, FL.